Liquid metal actuator driven by electrochemical manipulation of surface tension

Loren Russell, James Wissman, and Carmel Majidi

Articles you may be interested in

Liquid metal actuator driven by electrochemical manipulation of surface tension

Loren Russell,[1] James Wissman,[1,2] and Carmel Majidi[1]

[1]*Mechanical Engineering, Carnegie Mellon University, Pittsburgh, Pennsylvania 15213, USA*
[2]*Acoustics Division, Naval Research Lab, Washington, DC 20375, USA*

We examine the electrocapillary properties of a fluidic actuator composed of a liquid metal droplet that is submerged in electrolytic solution and attached to an elastic beam. The beam deflection is controlled by electrochemically driven changes in the surface energy of the droplet. The metal is a eutectic gallium-indium alloy that is liquid at room temperature and forms an nm-thin Ga_2O_3 skin when oxidized. The effective surface tension of the droplet changes dramatically with oxidation and reduction, which are reversibly controlled by applying low voltage to the electrolytic bath. Wetting the droplet to two copper pads allows for a controllable tensile force to be developed between the opposing surfaces. We demonstrate the ability to reliably control force by changing the applied oxidizing voltage. Actuator forces and droplet geometries are also examined by performing a computational fluid mechanics simulation using Surface Evolver. The theoretical predictions are in qualitative agreement with the experimental measurements and provide additional confirmation that actuation is driven by surface tension. *Published by AIP Publishing.*
https://doi.org/10.1063/1.4999113

Surface tension and capillary effects play a governing role in a variety of optoelectronic, microfluidic, and MEMS devices.[1,2] Examples range from capillary pumps in bioanalytical devices[3] to self-assembling microstructures that use reflowable solder to create out-of-plane microstructures.[4] An area of special interest has been to use surface tension within an actuator to perform mechanical work. Micro-conveyor systems have seen some of the most direct applications of electrically controllable and reversible forces to position small objects.[5,6] Other previously named "surface tension actuators" do not directly rely on capillary effects as the driving force and instead use them to stabilize or facilitate a non-fluidic motion.[7] Although many methods for controlling interfacial energies have been demonstrated (e.g., temperature,[8] light,[9] and electrowetting[10]), they have typically been employed to control individual liquid droplets. Electrowetting forces have previously been controlled and measured although droplets on the millimeter scale are limited to forces in the micronewton range.[11] While droplet manipulation plays an important role in certain microfluidic and optoelectronic systems, actuation through direct electrocapillary action could still have an impact in a much broader range of applications where reversible mechanical force is required.

Here, we introduce a technique to perform direct capillary actuation using electrochemical redox reactions. In contrast to most electroosmotics and electrowetting on dielectrics,[12,13] this approach requires relatively low voltage (∼1 V) and can be operated with conventional microelectronics. Rapid and reversible electrocapillary actuation is accomplished using a droplet of eutectic gallium indium (EGaIn), which is a non-toxic metal alloy that is liquid at room temperature and has been used for a variety of applications in soft microfluidic sensing and electronics.[14–18] Previously, it has been shown that the surface tension of EGaIn can be dramatically modulated by immersing a droplet in an aqueous electrolytic solution and applying a voltage bias of up to 2 V.[19,20] These applied voltages control the thickness of a Ga_2O_3 skin that forms on the surface of the droplet, which acts as a surfactant that separates the liquid metal from the surrounding solution. By controlling the applied voltage potential, the droplet's surface tension can vary from ∼500 mN/m to near zero. EGaIn electrochemistry has previously been used for fluidic pumping,[21,22] directed fluid motion,[23–25] mixing through chaotic advection,[26] a reconfigurable optical reflector,[27] and transistor-like switching.[28] While these studies explore a wide range of fluidic motions and electrocapillary responses, none directly examines the mechanical work performed by an EGaIn droplet between cycles of reduction and oxidation.

To characterize the force output, we use the testing setup presented in Fig. 1. The testbed contains an EGaIn droplet immersed in NaOH(aq) and wetted to a fixed pad and the tip of a cantilever. The droplet forms a liquid bridge[29] that exerts equal-and-opposite force on the opposing surfaces and causes the cantilever to bend in proportion to the voltage-controlled surface tension. In addition to experimental testing, the droplet deformation and capillary force exerted on the cantilever are examined by performing a computational fluid mechanics simulation using Surface Evolver (SE). This allowed us to confirm that the change in the droplet shape and capillary forces that we observed could be primarily explained by the interplay of surface tension and gravitational effects. Previous work has gone into even greater detail in relating the shape, capillary forces, and dynamics of liquid bridges[30–33] in response to surface tension and electric fields. Previous studies have also explored the dynamics of droplet formation in an electric field[34] and rate-dependent interactions with a solid surface.[35] However, for this study, we focused on static analysis with SE since this was adequate for examining the predominate fluid mechanics that govern the experimentally observed phenomenon.
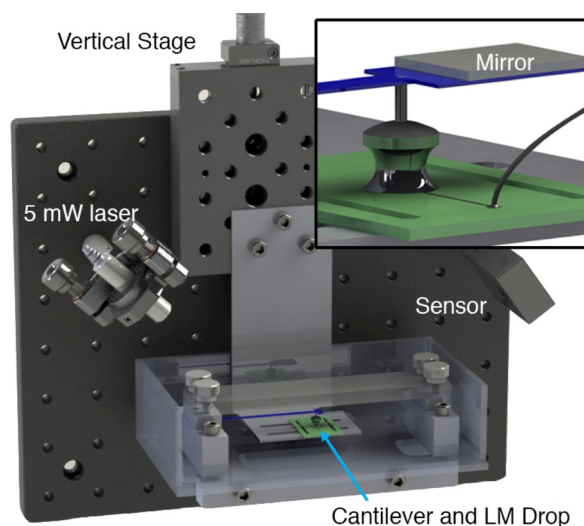
FIG. 1. Optical test stand for the force measurement; (inset) close-up of the free cantilever end and the EGaIn droplet.

A first order approximation of the force was also found by assuming that the droplet profile had a constant radius of curvature and following the equations provided by Streator for a liquid bridge between two fixed plates. The result of this analysis was within 10% of the measured and simulated values and helped to confirm that the underlying physics were in agreement with our measurements.

Electrocapillary response is measured using the optical test platform presented in Fig. 1. The EGaIn droplet exerts a tensile force on a Cu-coated pad which hangs off at the end of a fixed-free cantilever via an insulated wire. The wire is looped over the cantilever such that it does not transmit torques into the beam and allows the hanging pad to somewhat self-align with the fixed pad below. The deflection of the cantilever is proportional to the surface tension γ of the droplet and is measured by tracking the motion of a laser (MXD1230; Farhop) that reflects off a small mirror attached to the tip of the cantilever. It is assumed that for small deflections (<1 mm), the pad alignment and orientation do not change. The location of the reflected laser spot is tracked using a position sensing detector (PDP90A; Thorlabs). A quarter inch piece of acrylic acts as an optical window so that the uneven surface of the bath does not interfere with the transmission of the laser as it passes in and out of the fluid.

To calibrate the setup, known masses are hung from the same location that the droplet forces act through. From these calibration data, a linear fit is generated to correlate subsequent sensor readings with an equivalent mass or force. The vertical distance that the droplet spans between the cantilever and the lower pad can be adjusted by a micrometer stage (PT1; Thorlabs). The cantilever tip deflection is determined by first calibrating the setup by coupling the stage and the cantilever with an acetal clip. The tip is deflected in 25 μm steps as sensor readings are taken over a 0.5 mm range. With both the force and deflection calibrations and the stage height being controllable, it is possible to determine both the force and the distance between the copper pads.

The droplet, Cu pads, and cantilever are submerged in an aqueous solution of NaOH (3% by weight; unless otherwise stated). The base solution removes the bulk of the

Ga_2O_3 skin and increases the droplet surface tension to approximately 500 mJ/m^2.[19] The volume of EGaIn is produced via a syringe pump, and its mass was recorded via a milligram weigh scale before being placed in the solution via a pippet. Reduction and oxidation are controlled by applying a voltage drop across the stationary Cu pad below the droplet and a graphite counter electrode immersed at the corner of the bath. Voltage is controlled using a microcontroller (Arduino Uno) and motor driver (Pololu), and another controller and 16-bit analog-to-digital conversion (ADC) shield are used to collect the sensor and input voltage.

The experimental measurements are compared with the results from a computational fluid mechanics simulation performed using Surface Evolver (Ken Brakke, Susquehanna University[36]). The simulation uses a gradient descent algorithm to determine the static forces and droplet shape that minimizes potential energy arising from surface tension and gravity. An edge constraint pins the rim of the droplet at the top and bottom surfaces to a circular profile where the droplet is in contact with the Cu pads. Another constraint prevents the vertices from passing below the bottom pad or above the top one. The starting mesh is generated by progressively refining and evolving the surface five times. After this, vertex averaging and equi-angulation are performed, which helps to distribute the vertices evenly while attempting to preserve the internal volume. When a parameter is changed, either pad separation or surface energy, the surface is evolved 1000$\times$ and vertex averaged so that the change in system energy between evolutions is on the order of $\sim$100 nJ. When the change in energy reaches this cut-off value, the system is considered to have converged. The net vertical capillary force is calculated as the derivative of the potential energy at static equilibrium with respect to variations in the vertical position (height) of the cantilever-mounted pad. As the surface tension is adjusted and the surface is re-evolved, the shape of the droplet is exported as a .stl file and used to perform a qualitative comparison with profiles from the experimental setup. Again, it is important to emphasize that this simulation was performed to validate that the underlying physics were in general agreement with our experimental results.

A 0.25 g EGaIn droplet (40 mm^3) is capable of producing a tensile force up to 7.5 mN and can undergo redox reactions at a rate of up to 12 Hz. The peak force is reached when a positive voltage (0.2 V) is applied to the counter electrode relative to the droplet which is grounded. This reductive bias completely removes the oxide skin and causes the droplet to form a catenoid shape to reduce its surface area [Fig. 2(d)]. The surface energy of the droplet causes it to exert a tensile force on the tip of the cantilever, inducing a downward deflection. When the bias is reversed, the droplet oxidizes and sags downwards towards the lower pad. The corresponding drop in surface energy relieves the tensile force on the upper pad, which moves upwards as the cantilever straightens out.

Referring to Fig. 2(a), the capillary force exerted on the cantilever scales monotonically with applied voltage. The static force and input voltage were sampled over a range of 0 to -1.6 V. Unless otherwise stated, the initial pad displacement (i.e., separation between the bottom pad and the cantilever pad) was typically set to 2.5 mm although this distance will change slightly ($\sim$0.1 mm) as the cantilever flexes.
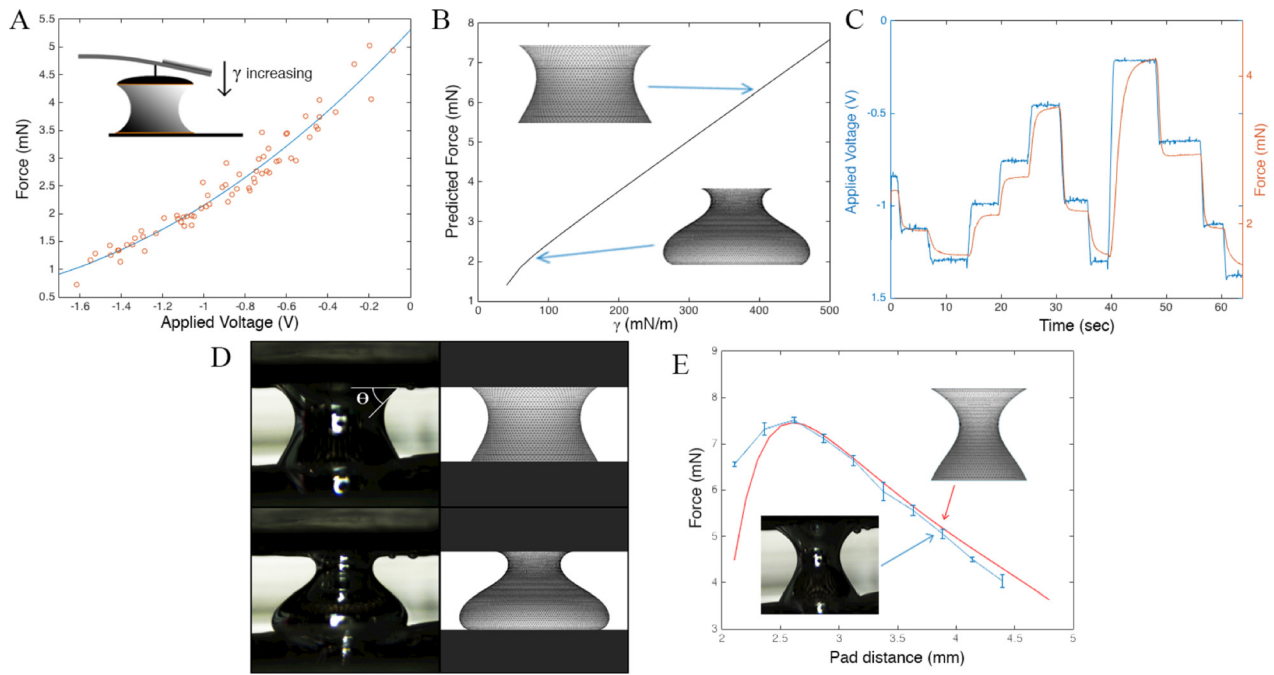
FIG. 2. (a) Measured vertical force as a function of applied voltage; the polynomial fit has an R^2 value of 0.95. (b) Theoretical prediction of force (computed in SE) as a function of surface tension. (c) Applied voltage and measured force versus time. (d) Comparison of the droplet shape with theoretical predictions obtained in SE for $\gamma = 400\,\text{mN/m}$ and $\gamma = 80\,\text{mN/m}$. (e) Comparison between experimental and simulated forces versus pad distance. A reducing voltage of 0.2 V was applied.

Fitting a second order polynomial yielded an R^2 value of 0.95 [Fig. 2(a)]. At voltages lower than $-1.6\,\text{V}$, the droplet will break contact with the top pad in a matter of seconds. Once this has occurred, even if the high surface is restored, the capillary bridge will not reform without manual intervention. This occurs because the spherical shape of the free droplet is not tall enough to contact the top pad. While for this application, complete droplet separation is not desirable, Wissman *et al.* have made use of this effect for field-controlled liquid metal switches.[28]

The experimental measurements in Fig. 2(a) are compared with predictions obtained using Surface Evolver (SE). The simulation was performed using the same dimensions ($40\,\text{mm}^3$ droplet volume, $5\,\text{mm}$ pad diameters), EGaIn density ($6.3\,\text{g/cm}^3$), and expected range of surface tensions (0–$0.6\,\text{J/m}^2$). A direct quantitative comparison is difficult since we do not have an accurate mapping between applied voltage and surface tension. Although this information has previously been produced by others,[19] it was not feasible to independently recreate these data within the scope of this work. Nonetheless, the theory and experiment appear to be in reasonable qualitative agreement. In particular, the theory captures the sagging of the droplet as the surface energy decreases. For relatively low surface energies below 30–40 mJ/m^2, the simulation tends to break down as extreme necking can lead to the intersection of multiple facets and non-physical results.

The simulation results from SE suggest an approximately linear relationship between force and surface tension [Fig. 2(b)]. Pairing this with the nonlinear plot of surface tension vs. voltage produced by Khan *et al.*[19] explains the trend shown in Fig. 2(a). By adjusting the input voltage [as shown in Fig. 2(c)], the effective surface tension can be tuned, which in turn directly affects the capillary force exerted by the droplet. This architecture is straightforward to control because the two primary components of the force, the internal Laplace pressure $\Delta P = \gamma \{R_1^{-1} + R_2^{-1}\}$ and vertical surface tension $T = 2\pi R_2 \gamma \sin\theta$ around the perimeter, scale with the surface tension γ.[29] Here, R_1 is the radius of curvature along the droplet profile, R_2 is the pad radius, and the contact angle θ is defined in Fig. 2(d). It should be noted that the force predicted in Fig. 2(b) is a "blocking force" that assumes a fixed pad height and does not take into account the deflection of the beam. This is based on the assumption that the beam deflection is small compared to the characteristic dimensions and displacements of the droplet. The testbed presented in Fig. 1 is also useful for understanding the effects that varying the pad distance has on the force from the liquid bridge.[30] At close distances, the droplet assumes a convex shape, which suggests a high internal pressure that pushes outwards on the contacting pads. As the pads move apart, the droplet forms a catenoid shape and the lower internal pressure contributes to an increase in net tensile force. Near droplet separation, the neck narrows and θ decreases, reducing the vertical force contribution from surface tension.

The forces reported by SE are consistently higher than those measured experimentally although the trends and shapes show reasonable qualitative agreement, as seen in Fig. 2(e). Error between the simulated and experimental results could be accounted for by imperfect pad alignment and wetting of the droplet as well as mechanical stresses present in the thin oxide layer.[37] Previous work has shown that the oxide layer can act to mechanically stabilize the droplet in shapes that would not otherwise be an energy minimum.[15] Future work would likely benefit from a more detailed characterization of the oxide thickness and its relation to the applied voltage. Techniques exist for studying the oxide thickness, and its mechanical properties have previously

been reported as well.[38,39] Combining this information would certainly add to the accuracy of future models.

Although the droplet can be commanded to a range of values while being oxidized, the settling time to reach a static value can take several seconds [Fig. 2(c)], which limits the ability to operate at higher frequencies. The frequency of actuation is controlled by the rate of electrochemical reduction and oxidation. During reduction (>0.2 V), the droplet moves rapidly ($\sim$20–40 ms) into its static equilibrium state under the force of surface tension. During oxidation, the dynamics of droplet deformation are governed by gravity, viscosity, and inertia and the motion is significantly slower. Because of this asymmetry in response speed, the actuator fails to smoothly track sinusoidal inputs. Instead, the actuator exhibits a more controlled response when subject to square waves with frequencies ranging from 1 to 12 Hz (Fig. 3). For frequencies of 12 Hz and below, the dynamic response of the actuator is governed by the natural frequency of the cantilever, which depends on its dimensions, density, and flexural rigidity. The natural frequency of the combined cantilever and droplet system was measured by plucking the cantilever and was found to be 7.5 Hz. This is within the range of frequencies (7–8 Hz) at which the amplitude of the actuator was observed to be greatest [see Fig. 3(b)].

At frequencies above 12 Hz, the amplitude becomes severely attenuated because there is inadequate time for the droplet to oxidize. The speed of oxidation can be increased by moving the counter-electrode closer, applying higher voltages, and increasing the concentration of charge carriers. However, this also results in a higher current (>50 mA) draw and greater production of gas bubbles. Placing multiple droplets in an antagonistic arrangement may allow for
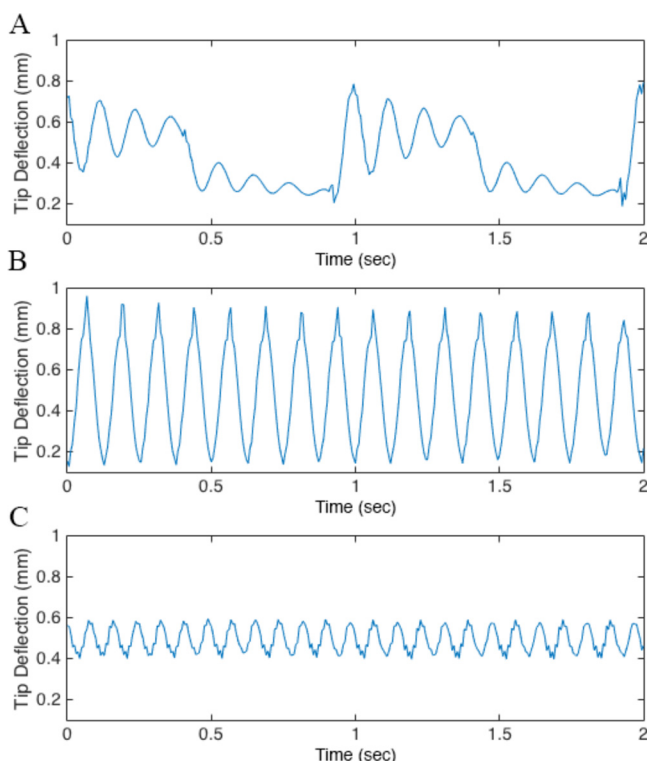
pulling in both directions and an increase in the output amplitude at higher frequencies. This would also eliminate the need for a cantilever to return the actuator to a default position. Without a built-in spring mass system, the passive dynamics would not be tied to a specific natural frequency other than that of the droplet itself, which may be desirable.

Preliminary estimates of the specific work and power densities for the EGaIn-based actuator can be obtained from the observed range of forces, displacements, and frequencies. During each cycle of actuation, the 0.25 g droplet undergoes displacements on the order of $\sim$1 mm. For larger pad displacements, the droplet may permanently separate during oxidation. For a peak force of 7.5 mN and an activation frequency of $\sim$10 Hz, this suggests a specific work (per cycle) and power outputs on the order of $\sim$10 μJ/g and $\sim$100 μW/g, respectively. Since capillary force scales with the droplet diameter, greater work and power densities are possible by replacing the 0.25 g droplet with an array of smaller droplets. For example, a 0.25 mg drop would have 1/10th the force output and maximum "stroke" displacement and therefore have a $10\times$ greater work density. Regardless, the current experimental results suggest that it is possible to harness the electrochemically reversible reduction and oxidation of EGaIn to power an actuator.

We examine the voltage-controlled mechanics of a liquid metal EGaIn droplet inside an electrolytic bath and explore the potential to harness its electrocapillary response for soft-matter actuation. An experimental testbed is introduced for measuring the shape of the droplet and the capillary force that it exerts during oxidation and reduction. The results are in reasonable qualitative agreement with predictions obtained using a computational fluid mechanics simulation. A more quantitative comparison could be possible if an accurate mapping between applied voltage, electrochemical reactions, and surface tension can be established. In particular, it would be useful to have experimental measurements that relate the thickness of the Ga_2O_3 skin to surface tension. Nonetheless, the results presented here show that the use of EGaIn for soft-matter actuation is promising. The preliminary estimates suggest that a 40 mm^3 droplet exhibits work and power densities on the order of $\sim$10 μJ/g and $\sim$100 μW/g, respectively. Greater values may be possible with an array of smaller droplets.

A key motivation for these experiments was to measure the forces and displacements that could be reliably generated and controlled through a liquid-metal bridge. The testbed architecture that we present is not intended to act as a standalone actuator but instead is designed to help to study the underlying electrocapillary properties of EGaIn. Capturing the force versus stroke profile and dynamic response will help to inform the design of subsequent EGaIn-based soft microfluidic actuators. Future work with this actuation mechanism will require improved management of the H_2 and O_2 gas bubbles that are formed during the redox reactions. This may necessitate the need for relief valves or alternative electrode materials, electrolytes, or claddings that produce non-gaseous electrochemical byproducts. Finally, future implementations could benefit from a more compact design with smaller droplets that exhibit a larger specific power density. Such actuators could be used for submersible and

FIG. 3. Response to the ± 1 V square wave for (a) 1 Hz, (b) 8 Hz, and (c) 12 Hz voltage input frequencies.

deformable robots, MEMS scale devices, and soft microfluidic valves or pumps.

[1] J. V. Collins, I. F. Lealman, P. J. Fiddyment, C. A. Jones, R. G. Waller, L. J. Rivers, K. Cooper, S. D. Perrin, M. Nield, and M. J. Harlow, Electron. Lett. **31**, 730 (1995).

[2] K.-S. Yun, I.-J. Cho, J.-U. Bu, C.-J. Kim, and E. Yoon, J. Microelectromech. Syst. **11**, 454 (2002).

[3] M. Zimmermann, H. Schmid, P. Hunziker, and E. Delamarche, Lab Chip **7**, 119 (2007).

[4] R. R. A. Syms, E. M. Yeatman, V. M. Bright, and G. M. Whitesides, J. Microelectromech. Syst. **12**, 387 (2003).

[5] Q. Ni, D. E. Capecci, and N. B. Crane, Sens. Actuators A: Phys. **247**, 579 (2016).

[6] I. Moon and J. Kim, Sens. Actuators A: Phys. **130–131**, 537 (2006).

[7] J. J. Sniegowski and E. J. Garcia, Proc. SPIE **2383** (1995).

[8] S. Daniel, M. K. Chaudhury, and J. C. Chen, Science **291**, 633 (2001).

[9] K. Ichimura, S.-K. Oh, and M. Nakagawa, Science **288**, 1624 (2000).

[10] G. Beni and S. Hackwood, Appl. Phys. Lett. **38**, 207 (1981).

[11] Q. Ni, D. E. Capecci, and N. B. Crane, Microfluid. Nanofluid. **19**, 181 (2015).

[12] J.-H. Change, D. Y. Choi, S. Han, and J. J. Pak, Microfluid. Nanofluid. **8**, 269 (2010).

[13] S. Zeng, C.-H. Chen, J. C. J. Mikkelsen, and J. G. Santiago, Sens. Actuators B: Chem. **79**, 107 (2001).

[14] S. Cheng and Z. Wu, Lab Chip **12**, 2782 (2012).

[15] M. D. Dickey, ACS Appl. Mater. Interfaces **6**, 18369 (2014).

[16] M. Dickey, Adv. Mater. **29**, 1606425 (2017).

[17] I. D. Joshipura, H. R. Ayers, C. Majidi, and M. D. Dickey, J. Mater. Chem. C **3**, 3834 (2015).

[18] T. Liu, P. Sen, and C.-J. Kim, J. Microelectromech. Syst. **21**, 443 (2012).

[19] M. R. Khan, C. B. Eaker, E. F. Bowden, and M. D. Dickey, Proc. Natl. Acad. Sci. **111**, 14047 (2014).

[20] J. Zhang, L. Sheng, and J. Liu, Sci. Rep. **4**, 7116 (2014).

[21] S.-Y. Tang, K. Koshmanesh, V. Sivan, P. Petersen, A. P. O'Mullane, D. Abott, A. Mitchell, and K. Kalantar-zadeh, Proc. Natl. Acad. Sci. **111**, 3304 (2014).

[22] R. C. Gough, A. M. Morishita, J. H. Dang, W. Hu, W. A. Shiroma, and A. T. Ohta, IEEE Access **2**, 874 (2014).

[23] R. C. Gough, J. H. Dang, M. R. Moorefield, G. B. Zhang, L. H. Hihara, W. A. Shiroma, and A. T. Ohta, ACS Appl. Mater. Interfaces **8**, 6 (2016).

[24] S.-Y. Tang, Y. Lin, I. D. Joshipura, K. Khoshmanesh, and M. D. Dickey, Lab Chip **15**, 3905 (2015).

[25] J. Zhang, Y. Yao, L. Sheng, and J. Liu, Adv. Mater. **27**, 2648 (2015).

[26] S.-Y. Tang, V. Sivan, P. Petersen, W. Zhang, P. D. Morrison, K. Kalantar-zadeh, A. Mitchell, and K. Khoshmanesh, Adv. Funct. Mater. **24**, 5851 (2014).

[27] A. F. Chrimes, K. J. Berean, A. Mitchell, G. Rosengarten, and K. Kalantar-zadeh, ACS Appl. Mater. Interfaces **8**, 3833 (2016).

[28] J. Wissman, M. D. Dickey, and C. Majidi, "Field-controlled electrical switch with liquid metal," Adv. Sci. (in press).

[29] J. L. Streator, *Surface Energy* (InTech, 2015).

[30] M. A. Fortes, Rev. Port. Qum **23**, 47 (1981), available at http://www.spq.pt/magazines/RPQuimica/303/article/994/pdf.

[31] D. N. Mazzone, G. I. Tardos, and R. Pfeffer, Colloid Interface Sci. **113**, 544 (1986).

[32] J.-B. Valsamis, M. Mastrangeli, and P. Lambert, Euro. J. Mech. Fluids **38**, 47 (2013).

[33] A. Klingner, J. Buehrle, and F. Mugele, Langmuir **20**, 6770 (2004).

[34] P. K. Notz and O. A. Basaran, J. Colloid Interface Sci. **213**, 218 (1999).

[35] X. Zhang and O. A. Basaran, J. Colloid Interface Sci. **187**, 166 (1997).

[36] K. A. Brakke, Exp. Math. **1**, 141 (1992).

[37] Q. Xu, N. Oudalov, Q. Guo, H. M. Jaeger, and E. Brown, Phys. Fluids **24**, 063101 (2012).

[38] M. Regan, H. Tostman, P. Pershan, O. Mangnussen, E. DiMasi, M. Ocko, and M. Deutsch, Phys. Rev. B **55**, 10786 (1997).

[39] R. J. Larsen, M. M. Dickey, G. M. Whitesides, and D. A. Weitz, J. Rheol. **53**, 1305 (2009).